DOI: 10.1002/ejic.200700010

Synthesis and Coordination Behavior of Symmetrical Tetraamine Phosphinic Acids

Vojtěch Kubíček,*[a] Ivan Řehoř,[a] Jana Havlíčková,[a] Jan Kotek,[a] Ivana Císařová,[a] Petr Hermann,[a] and Ivan Lukeš[a]

Keywords: Aminophosphinates / Complexes / Stability constants / Potentiometry

Two new tetraamine ligands, bis[*N*-(2-aminoethyl)aminomethyl]phosphinic acid (Hen_2p) and bis[*N*-(3-aminopropyl)-aminomethyl]phosphinic acid (Hpn_2p), were synthesized from the corresponding diaminoalkanes and bis(chloromethyl)phosphinic acid. Their acid–base properties and complexation with Cu^{2+}, Ni^{2+}, and Zn^{2+} ions were studied by potentiometric titrations. Different chain lengths of the ligands result in significantly different coordination abilities. The five-membered chelate ring of Hen_2p leads to a higher stability of its complexes. In comparison with tetraamines having the same number of the bridging atoms separating the amino groups, the presence of the phosphinic acid moiety decreases the basicity of the amine groups, and consequently, the stability of their complexes. Several solid-state structures were determined by X-ray diffraction analysis. Four nitrogen atoms coordinate the Cu^{2+} or Zn^{2+} ion in a square-planar fashion, whereas the phosphinic acid group is not coordinated or acts as a bridging unit between neighboring metal ions. The unexpectedly high stability of the Ni^{2+}/Hpn_2p complex can be explained by the possible presence of a tetramer in solution as was found in the solid state.

Introduction

The phosphinic acid group is derived from phosphoric acid by replacement of two –OH groups with hydrogen, alkyl, or aryl groups (Figure 1). In comparison with phosphonates (where only one –OH group is replaced), phosphinic acid derivatives are less studied because their synthesis is more complicated. Derivatives of phosphonic and phosphinic acids substituted in the α-position with an amino group have been intensively studied over the last 25 years as inhibitors of various enzymes.[1] Tetrahedral phosphinic (or phosphonic) acid groups mimic a transition state that is present during the hydrolysis of peptides and block efficiently the active sites of hydrolytic enzymes. Hydrolytic enzymes such as, for example, peptidases often contain a metal ion in the active site, and the inhibiting aminophosphinic acid binds the metal ion. Therefore, complexation properties of the phosphorous acid analogs have been studied in solution as well in the solid state.[2,3] Some of these compounds are produced commercially in a large scale as herbicides (Glyphosate, Bialaphos, etc.).[4]

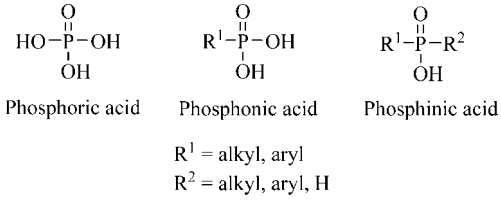

Figure 1. Phosphoric acid and its organophosphorus analogues.

Usually, an introduction of acidic fragments into a chelating molecule results in a higher stability of the complexes and decreases the overall charge of the complex formed in comparison with those of the corresponding amine. Phosphonic or phosphinic acid groups represent an alternative for the generally used carboxyl group. Relative to the carboxylate function, the presence of the phosphinic acid group decreases the basicity of the nearest amino group as well as the stability of the complexes as a result of the electron-withdrawing effect of the phosphorus atom. In the case of phosphonic acid derivatives, the doubly negative charge of the phosphonate overcompensates this disadvantage, leading to higher dissociation and, consequently, stability constants. Dissociation constants of the nitrogen atoms and stabilities of the complexes of these related ligands then follow the order: aminophosphinates < aminocarboxylates < aminophosphonates.[2,3] On the other hand, the higher acidity of the phosphonic and phosphinic acid groups causes the complexation to start at a lower pH. The lower stability

[a] Department of Inorganic Chemistry, Faculty of Science, Charles University in Prague,
Hlavova 8, 128 40 Prague 2, The Czech Republic
E-mail: vvvojta@volny.cz

Supporting information for this article is available on the WWW under http://www.eurjic.org or from the author.

of the phosphinate complexes can by compensated by their structural flexibility. Whereas the carboxylic and phosphonic acid groups are the terminal ones, the phosphinic acid group allows the attachment of another molecule fragment and the formation of more complicated structures and bifunctional ligands. Studies of phosphinic acid analogs of common amino acids in solution are not very frequent and confirm the above general considerations.[5–9] In addition, the solution properties depend on the kind of substituent bound to the phosphorus atom for simple aminophosphinic acids[8] as well as for their dipeptides.[10] In the complexes in the solid state, the amino group can be protonated and the metal ion is bound only by the phosphinate oxygen atom(s)[9,11–15] or the phosphinic amino acids can behave as chelating ligands bound through amino and phosphinate groups.[8,9,16,17] In addition, the phosphinate moiety serves as a bridge between two metal ions, often forming characteristic eight-membered M–(O–P–O)$_2$–M metallacycles.[8,11,13–15]

During the last decades, aminoalkylphosphinic acid groups have been used as building blocks in the design of polydentate ligands.[2,18] These compounds, usually based on acyclic[19–22] or macrocyclic[23–29] polyamine skeletons, have been studied as ligands for binding of "hard" metal ions, e.g. lanthanide(III) ions. The introduction of the methylphosphinic acid group(s) into DTPA or DOTA skeletons has led to an interesting alteration of properties of complexes of such ligands which are studied as possible contrast agents in magnetic resonance imaging,[30–37] for utilization in nuclear medicine,[38] or for luminescence imaging.[39]

Surprisingly, complexation abilities of compounds bearing two aminoalkyl substituents on one phosphorus atom have been only sparingly investigated. There are only several studies dealing with the solution[9,40–42] or solid-state[9,41,42] studies of this class of ligands. To obtain more information about the ligands, we decided to synthesize and investigate two new symmetrical polyaminophosphinic acid ligands, bis[*N*-(2-aminoethyl)aminomethyl]phosphinic acid (Hen$_2$p) and bis[*N*-(3-aminopropyl)aminomethyl]phosphinic acid (Hpn$_2$p) (Figure 2). Their acid–base and complexation properties were studied by using potentiometric titrations and UV/Vis spectroscopy. The solid-state structures of several complexes were determined by X-ray diffraction. As ligands containing the phosphinic acid group inside a macrocyclic skeleton have been previously prepared,[43] these open-chain ligands can serve for comparison of the properties of the corresponding cyclic and acyclic ligands.

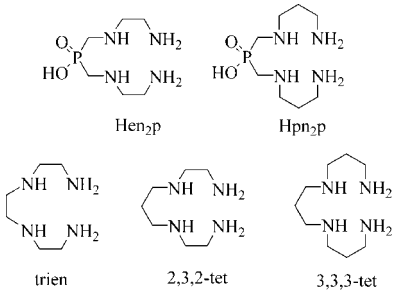

Figure 2. Ligands discussed.

Results and Discussion

Synthesis

The ligands Hen$_2$p and Hpn$_2$p were prepared by reaction of bis(chloromethyl)phosphinic acid (**1**) with 1,2-diaminoethane or 1,3-diaminopropane. Nucleophilic substitution of the chlorine atoms proceeds in almost quantitative yield. The formation of polymers was reduced by using a 100-fold excess of the diaminoalkane. After purification on ion-exchange resins, both ligands were isolated as their trihydrobromides; they slowly lost hydrobromic acid on storage or heating.

Neither the two ligands nor their salts are soluble in common organic solvents. For future synthetic purposes, solubility in organic solvents would be useful. Therefore, we tried to prepare an esterified form **3** by the reaction of isopropyl bis(chloromethyl)phosphinate (**2**) with the diaminoalkanes (Scheme 1). All these attempts failed, as the deesterification (by alkylation of the diaminoalkane with the isopropyl group) proceeded much faster than the substitution of chlorine atoms, and, at reflux temperature, both ligands were formed in the nonesterified form. When the reaction mixture was stirred at ambient temperature, the only product formed was bis(chloromethyl)phosphinic acid (**1**) as a result of the deesterification.

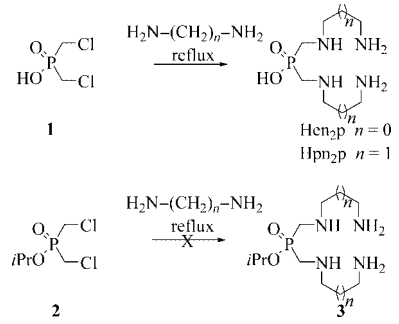

Scheme 1. Synthesis of the ligands.

Acid–Base Properties

Both ligands, Hen$_2$p and Hpn$_2$p, contain five groups that can be protonated. The last two dissociations occur in strongly alkaline solution. The protonation constants, corresponding to proton loss from the terminal (primary) amino groups, are similar to those found in the corresponding tetraazaalkanes (Table 1). Whereas these two deprotonations are almost independent, the other two dissociations are strongly affected by the number of atoms separating the secondary amino groups from already protonated primary amino groups. The presence of propylene bridges results in a higher basicity of the secondary amino groups. In the case

Table 1. Dissociation constants of the ligands Hen_2p, Hpn_2p, and linear tetraamines.[44]

	Hen_2p	Hpn_2p		trien[a]	Hen_2p	2,3,2-tet[b]	Hpn_2p	3,3,3-tet[c]
$\log\beta_1$	10.10(2)	10.60(1)	$pK_A(HL)$	9.95	10.10	10.25	10.60	10.46
$\log\beta_2$	19.36(2)	20.48(1)	$pK_A(H_2L)$	9.31	9.26	9.5	9.88	9.82
$\log\beta_3$	25.06(2)	27.89(2)	$pK_A(H_3L)$	6.86	5.70	7.28	7.41	8.54
$\log\beta_4$	29.25(3)	33.78(2)	$pK_A(H_4L)$	3.66	4.19	6.02	5.89	7.22
$\log\beta_5$	–	–	$pK_A(H_5L)$	–	<1	–	<1	–

[a] trien = triethylenetetraamine (1,4,7,10-tetraazadecane). [b] 2,3,2-tet = 1,4,8,11-tetraazaundecane. [c] 3,3,3-tet = 1,5,9,13-tetraazatridecane).

of ligands Hen_2p and Hpn_2p, these two dissociation constants were found to be 1–2 orders of magnitude lower than those found for 2,3,2-tet and 3,3,3-tet. This decrease in basicity is typical for amino groups in the α-position to the phosphinate moiety.[2,3,9] Protonation of the phosphinate group occurs at very low pH (<1). The values of the dissociation constants of the fully protonated species are below the limit of the potentiometric method, and it was therefore not possible to calculate these constants.

Complexation Properties

To simplify the following text we use a three-digit code for describing the complexes. The first digit represents the number (stoichiometric coefficient) of protons, the second one is the number of ligand molecules, and the third one is the number of metal ions. The negative value of the first digit represents a hydroxido complex. In general, complex $[H_hL_lM_m]$ is represented by [hlm], and its overall stability constant is β_{hlm}. Charges of the complexes are omitted.

Complexation properties of the ligands Hen_2p and Hpn_2p towards Cu^{2+}, Ni^{2+}, and Zn^{2+} ions were studied by potentiometric titrations. The results are listed in Table 2. Some of the constants were not calculated. This is probably due to a simultaneous protonation of two sites and/or a very low abundance of the corresponding species (<10%).

Table 2. Overall stability constants ($\log\beta_{hml}$) of the complexes.

Coefficient			Cu^{2+}		Ni^{2+}		Zn^{2+}	
h	*l*	*m*	Hen_2p	Hpn_2p	Hen_2p	Hpn_2p	Hen_2p	Hpn_2p
3	1	1	–	31.50(6)	–	30.04(9)	–	–
2	1	1	–	27.83(1)	–	24.05(3)	–	23.17(4)
1	1	1	24.17(2)	22.00(3)	19.60(2)	17.88(4)	–	–
0	1	1	21.63(2)	15.94(1)	15.68(1)	11.34(1)	12.04(1)	8.22(5)
– 1	1	1	–	–	–	–	1.36(3)	–1.99(3)
3	2	1	–	–	–	41.73(6)	–	40.01(2)
2	2	1	47.76(5)	–	38.67(8)	–	34.29(5)	32.51(4)
1	2	1	–	30.50(9)	29.56(5)	–	–	–
0	2	1	26.45(9)	19.94(7)	–	13.91(7)	15.84(7)	11.92(6)
0	1	2	–	20.76(2)	–	13.61(5)	14.09(4)	–
– 1	1	2	–	13.16(4)	–	–	–	4.27(1)
– 2	1	2	–	5.79(2)	–	–	–	–

Ligand Hen_2p

In equimolar solutions, complexation of the Cu^{2+} and Ni^{2+} ions starts with formation of the monoprotonated

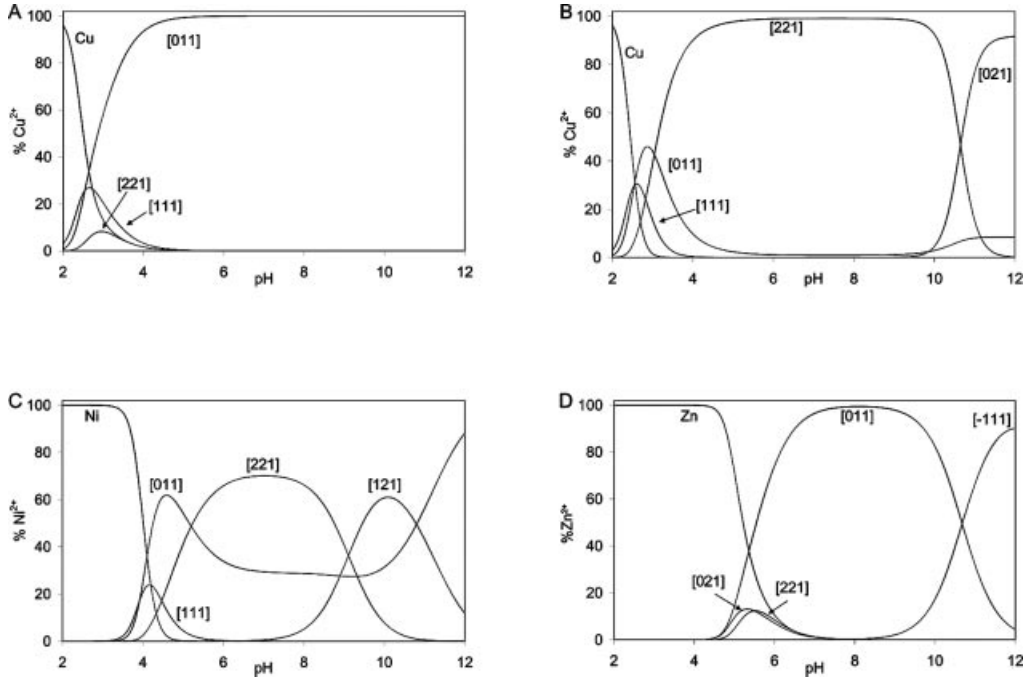

Figure 3. Distribution diagrams. (A) Cu^{2+}/Hen_2p 1:1; (B) Cu^{2+}/Hen_2p 1:2; (C) Ni^{2+}/Hen_2p 1:2; (D) Zn^{2+}/Hen_2p 1:1.

[111] complex at pH ≈ 2 for Cu^{2+} (Figure 3A) and pH ≈ 3 for Ni^{2+}. The protonated complex does not exhibit a high abundance (<30%), and its deprotonation to the [011] species occurs with low pK_A (pK_{Cu} = 2.5, pK_{Ni} = 3.9). The nonprotonated complex [011] is the only species present in the neutral and alkaline regions. Complexation of the Zn^{2+} ion proceeds differently. The protonated complex [111] was not observed. Complexation starts at pH ≈ 4.5 with the formation of the [011] complex. At pH > 8, the hydroxido [–111] complexes are formed and become the main species present in the solution under the strongly alkaline conditions (Figure 3D).

In the presence of excess ligand (1:2 M^{2+}/L ratio), [221] complexes were formed in the neutral region (abundance >90% for Cu^{2+}, ca. 70% for Ni^{2+}, ca. 40% for Zn^{2+}; Figure 3B, C). Deprotonation results in the formation of [021] complexes (Cu^{2+}, Zn^{2+}) at pH ≈ 10–11 or a [121] complex (Ni^{2+}) at pH ≈ 9. In the presence of excess metal (2:1 M^{2+}/L ratio), the M^{2+} hydroxides precipitated in all systems. Distributions in all systems are given in the Supporting Information (Figure S1).

Ligand Hpn_2p

A successful fitting of titrations of all three studied systems containing the ligand Hpn_2p required inclusion of the complexes with M/L ratios 1:1, 1:2, and 2:1 in various degrees of protonation (Figure 4). The complexation process starts at slightly higher pH (about 0.5 units) than that for Hen_2p. Complexation of Cu^{2+} and Ni^{2+} ions exhibits a preference for formation of the [011] complex, which is the main species present in equimolar solution (Figure 4A, B). In the presence of excess ligand, the complexes with 1:2 M^{2+}/L stoichiometry are formed only in the case of Cu^{2+} ion in alkaline solutions (pH > 9). In the case of Ni^{2+}, complex [011] remains the major species in the whole alkaline region (Figure 4C). In the presence of excess Cu^{2+} ions, the dinuclear [012] complex becomes dominant with an abundance of ca. 90% (at pH ≈ 6). For Ni^{2+}, the abundance of the [012] complex does not reach more than 30%. The Zn^{2+}/Hpn_2p system involves a mixture of several complexes with comparable abundances in equimolar solution and with ligand in excess. In the presence of excess Zn^{2+} ions, the dinuclear [–112] hydroxido complex becomes a major species. The unusually high abundance of this complex in equimolar solution (ca. 50% at pH ≈ 8) indicates a strong preference for this species (Figure 4D), where OH^- probably forms a bridge between two metal ions. A similar motif of two hydroxide-bridged zinc(II) ions was observed in several types of metalloenzymes[45] and artificial catalytic centers[46] playing a role in hydrolytic processes. Distributions in all systems are given in the Supporting Information (Figure S2).

Results of the potentiometric study show that both studied ligands exhibit similar trends of coordination behavior to that of related linear tetraamines (Table 3). Stability constants of complexes of the tetraamine ligands with divalent metals increase in the order 3,3,3-tet < trien < 2,3,2-tet as a result of steric properties of the ligand. The least stable complexes are formed by 3,3,3-tet as all chelate rings in the complexes are six-membered, which is in general less convenient relative to trien and 2,3,2-tet, which form five-membered chelate rings.[47] The flexibility of the propylene bridge in 2,3,2-tet allows the formation of complexes having ideal square geometry, whereas the shorter ethylene bridge of trien is not ideal for this equatorial coordination. The lower basicity of Hen_2p and Hpn_2p in comparison with those of 2,3,2-tet and 3,3,3-tet (ligands having the same

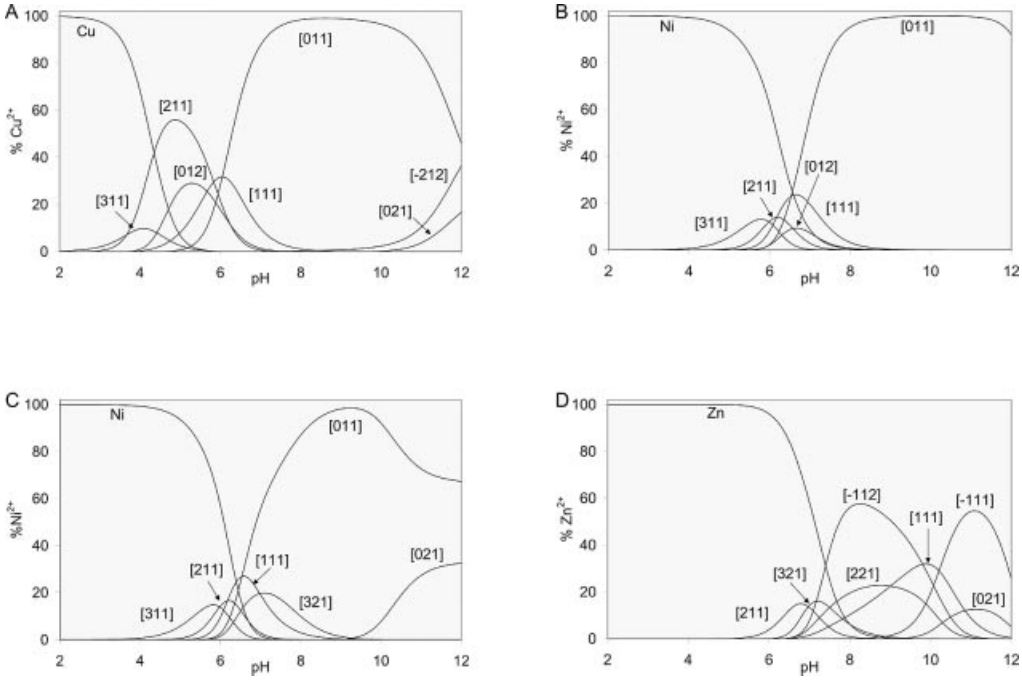

Figure 4. Distribution diagrams. (A) Cu^{2+}/Hpn_2p 1:1; (B) Ni^{2+}/Hpn_2p 1:1; (C) Ni^{2+}/Hpn_2p 1:2; (D) Zn^{2+}/Hpn_2p 1:1.

number of bridging atoms between amino groups) results in the decrease of the stability constants of the [011] complexes, which are 1–3 units lower than those reported for the corresponding tetraamines. The only exception is the Ni^{2+}/Hpn_2p system, whose [011] complex exhibits a slightly higher stability than that of 3,3,3-tet. This can be explained by a possible formation of the cyclic tetrameric complex [044], which was identified in the solid state (see further). As this complex shows very similar potentiometric behavior to the [011] complex, the presence of the [044] complex cannot be confirmed by potentiometry, mainly because of the rather complex chemical model of the system. The possible presence of the tetramer in the solution is supported by the similarity of the UV/Vis spectra in the solution (Ni^{2+}/Hpn_2p 1:1, pH = 10, 100% abundance of [011] species according to the distribution diagram, see Figure 4B) and in the solid state (complex [044], see crystallographic part). The UV/Vis spectra are shown in Figure 5 (maxima in the solution at 364, 581, and 947 nm; maxima in the solid state at 366, 587, and 970 nm).

Table 3. Comparison of stability constants $\log\beta_{011}$ of complexes found for Hen_2p and Hpn_2p with those reported for linear tetraamines.[44]

Ion	Hen_2p	Hpn_2p	trien[a]	2,3,2-tet[b]	3,3,3-tet[c]
Cu^{2+}	21.63	15.94	20.2	23.9	17.3
Ni^{2+}	15.68	11.34	14.4	16.4	10.65
Zn^{2+}	12.04	8.22	12.1	12.8	9.41

[a] trien = triethylenetetraamine (1,4,7,10-tetraazadecane). [b] 2,3,2-tet = 1,4,8,11-tetraazaundecane. [c] 3,3,3-tet = 1,5,9,13-tetraazatridecane.

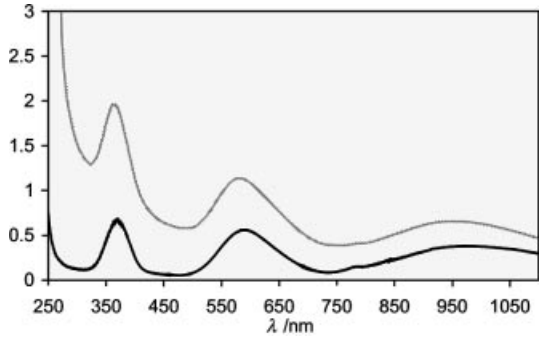

Figure 5. Comparison of the UV/Vis spectra of the $[Ni_4(pn_2p)_4]^{4+}$ complex in solution (dashed line) and in the solid state (solid line). The *y* axis shows absorbance units for solution and Kubelka–Munk units for the solid state.

Comparison of the Hen_2p and Hpn_2p systems can nicely document the different selectivity of these ligands. The higher stability of Hen_2p complexes and the simpler models for the M^{2+}/Hen_2p systems (4–5 species, strong preference for [011] complexes) indicate that the stereochemical properties of this ligand are much more suitable for the complexation of the studied divalent metal ions than those of the ligand Hpn_2p (7–9 species in each system).

Crystallography

The crystal structures of three salts of the H_4en_2p cation, two Hen_2p and two Hpn_2p complexes were determined by X-ray diffraction. In contrast to the simplest bis(aminomethyl)phosphinic acid,[9] the phosphinic acid groups of the studied ligands are not coordinated in acid solution, and the ligand behaves only as an organic base. In the presence of a bulky anion, e.g. tetrachlorocuprate(II), the simple salts crystallize. In neutral and alkaline solutions, both ligands behave in a similar manner as the corresponding tetraamines; four nitrogen atoms of one ligand molecule are coordinated in equatorial positions around the transition-metal ion. In the solid state, the phosphinic acid group is mostly coordinated to another metal center and plays the role of the bridging unit. In simple systems [ligand, metal(II) chloride, hydrochloric acid, sodium hydroxide], crystallization experiments were not successful – oily and glassy products were formed. Single crystals were obtained after bulky anions (perchlorate, hexafluorophosphate) and ammonium cations (forming a hydrogen-bond network) were added and the pH was adjusted to the value of the maximum abundance of the species in solution (according to the distribution diagrams). In addition, in most cases, only several single crystals, which decomposed on standing in air, were obtained. Therefore, microanalytical data are not provided (the rest of the solution formed only oils).

Ligand Salt Structures (4, 5, 6)

In all three structures, all four amino groups are protonated, and the phosphinic acid group is deprotonated. The distances between the phosphorus atom and the two oxygen atoms in the structure of $(H_4en_2p)Cl_3$ (**4**) are the same (1.49 Å), which indicates full delocalization of the phosphinate negative charge. The two side arms of the ligand are almost planar. Both compounds $(H_4en_2p)[CuCl_4]Cl$ (**5**) and $(H_4en_2p)[ZnCl_4]Cl$ (**6**) are almost isostructural. All amino groups are protonated, whereas the phosphinic acid group is deprotonated. In contrast to the structure of **4**, the ligand side-arms are not arranged in one plane. Torsion angles around the phosphorus atom (C–P–C–N) are 73–75° (for **4**), 155–158° (for **5**), and 160° (for **6**). The torsion angles about the P–C–N–C bonds are antiperiplanar (170–180°). Other bonds in the chain are in the synclinal conformation (torsion angles of 61–82°) probably because of the presence of the hydrogen-bond network between the protonated amino groups and the anions. The coordination sphere of both tetrachloroanions is a distorted tetrahedron. The structure of the $(H_4en_2p)^{3+}$ cation in $(H_4en_2p)Cl_3$ (Figure S3), the independent unit found in the crystal structure of $(H_4en_2p)[CuCl_4]Cl$ (Figure S4), and selected geometric parameters (Table S1) are given in the Supporting Information.

$Na_2(NH_4)_4[Cu(en_2p)]_4Br_4(PF_6)_6\cdot H_2O$ (7)

The structural unit has a plane of symmetry. The structurally independent part consists of four halves of the complex molecules. Their central atoms (Cu^{1a}, Cu^{1b}, Cu^{1c}, and

Cu^{1d}) are situated in a plane. Three complex units (with central ions Cu^{1a}, Cu^{1b}, and Cu^{1c}) are coordinated to one Na^+ cation (Na^1) through phosphinate oxygen atoms. The fourth complex forms a coordination bridge between Cu^{1b} and $Cu^{1c\#}$ (of the neighboring crystal unit) through the two bromide anions Br^2 and Br^3. In all complexes, amino groups occupy equatorial positions, and the N_4Cu plains are perpendicular to the crystallographic plane of symmetry. The Cu^{2+} ions Cu^{1a} and Cu^{1b} have an octahedral coordination sphere with one bromide anion (Br^1 or Br^2) and one phosphinate oxygen atom (O^{61b} or O^{61c} coming from ligand molecules coordinated to the neighboring Cu^{2+} ions) in axial positions. The coordination sphere of Cu^{1c} is square-pyramidal with bromide anion $Br^{3\#}$ in the axial position. Cu^{1d} has an octahedral coordination sphere with two bromide anions (Br^2 and Br^3) in the axial position. Part of the crystal structure of complex **7** is shown in Figure 6. Cocrystallized water molecules as well as ammonia cations fill the empty cavities of the structure, forming a system of hydrogen bonds. The remaining spaces in the coordination sphere of the Na^+ ion are occupied by fluorine atoms of the hexafluorophosphate anion, phosphinate oxygen atoms O^{61a}, O^{61d}, O^{62d}, and the bromide ion Br^4. Selected geometric parameters are given in the Supporting Information (Table S2).

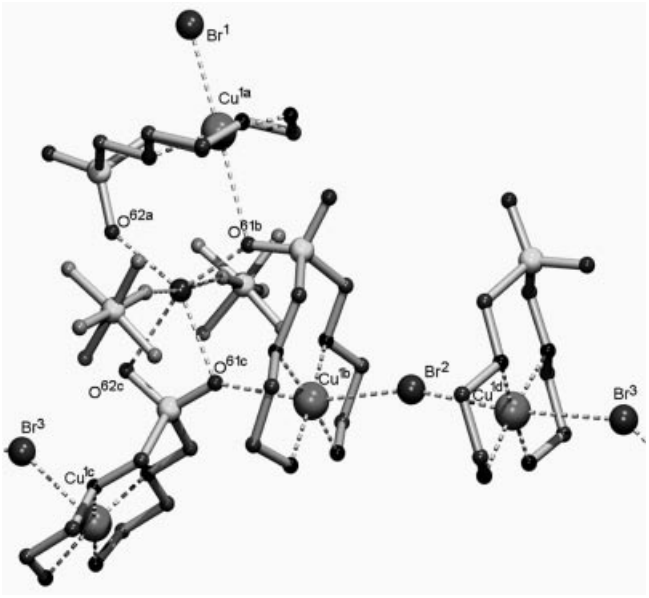

Figure 6. Complex framework found in the crystal structure of $Na_2(NH_4)_4[Cu(en_2p)]_4Br_4(PF_6)_6{\cdot}H_2O$ (**7**).

$Na_{3/2}(NH_4)_2[Zn(en_2p)]_3Br_{5/2}(PF_6)_4{\cdot}3H_2O$ (8)

The structural unit has a plane of symmetry. Three halves of complex molecules form an independent part. Three central atoms (Zn^{1a}, Zn^{1b}, and Zn^{1c}) form three vertexes of the virtual square at the center of which is the Na^+ ion Na^1. The N_4Zn planes in all complexes are perpendicular to the plane of symmetry. The first complex (Zn^{1a}) shows tetragonal pyramidal geometry. The axial position is occupied by the bromide anion Br^{1a}. The distance to another bromide anion Br^1 is too long (3.22 Å) to expect there to be a direct coordination bond in the remaining axial position. Zn^{1b} has octahedral geometry. The axial positions are occupied by the phosphinate oxygen atom O^{61a} and bromide anion Br^2. The bromide anion Br^2 plays the role of bridging ligand and it is coordinated to the atom $Zn^{1b\#}$ from the neighboring trimeric unit. The third complex molecule whose central atom is Zn^{1c} has tetragonal pyramidal geometry with the phosphinate oxygen atom O^{61b} in the axial position. Similarly to the first complex molecule, there

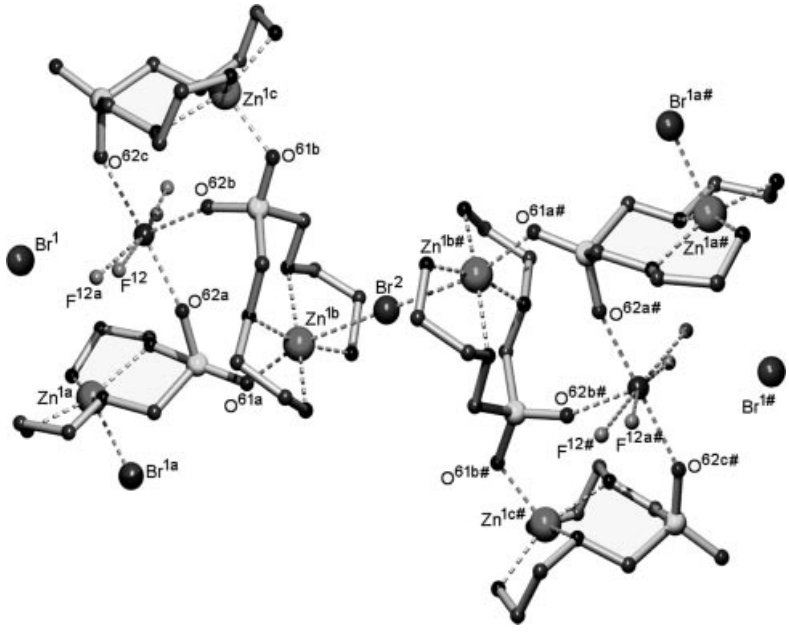

Figure 7. Complex framework found in the crystal structure of $Na_{3/2}(NH_4)_2[Zn(en_2p)]_3Br_{5/2}(PF_6)_4{\cdot}3H_2O$ (**8**). Two structural units are displayed. Fluorine atoms coordinated to the Na^+ ion belong to the hexafluorophosphate anions.

is a bromide anion ($Br^{1\#}$) in the direction of the second axial position, but too far from the metal center to be assigned as directly coordinated (3.23 Å). The square-pyramidal coordination sphere of the Na^+ ion Na^1 is occupied by three phosphinate oxygen atoms (O^{62a}, O^{62b}, and O^{62c}) and two fluorine atoms coming from hexafluorophosphate anions. Other PF_6^-, NH_4^+, and Br^- ions are bound into the structure by a framework of hydrogen bonds. The framework of the complex molecules found in the crystal structure of **8** is shown in Figure 7. Selected geometric parameters are given in the Supporting Information (Table S3).

$Na_2[Cu(pn_2p)]_4Br_2(ClO_4)_4\cdot 3H_2O$ (9)

The structural unit has again a plane of symmetry. Four halves of the complexes (with central atoms Cu^{1a}, Cu^{1b}, Cu^{1c}, and Cu^{1d}) form an independent unit. The copper atoms are located in the corners of the virtual square at whose center is the Na^1 atom. The motif of four nitrogen atoms in the equatorial plane of the complexes is similar with that found in the previous structures; ligand equatorial planes are perpendicular to the crystallographic plane of symmetry. The coordination spheres of Cu^{1a} and Cu^{1b} have tetragonal pyramidal geometry, where the axial position is occupied by a phosphinate oxygen atom (O^{71b} and O^{71c}, respectively) coming from the neighboring complex. The octahedral coordination sphere of the Cu^{1c} atom is completed in the axial positions with the bromide anion Br^{1c} and the disordered phosphinate oxygen atom O^{71d} coming again from the neighboring complex unit. The trimethylene bridge of the ligand exhibits disorder into two positions. The last complex unit Cu^{1d} has square-pyramidal geometry whose axial position is occupied by the oxygen atom of a water molecule, O^{1d}. The octahedral coordination sphere of the Na^1 consists of four oxygen atoms from four phosphinate groups in the equatorial plane (O^{72a}, O^{72b}, O^{72c}, and O^{72d}). Oxygen atoms coming from perchlorate anions occupy the axial positions. Cocrystallized water molecules and bromide anions are fixed in the structure by the hydrogen-bond network. The complex framework found in the crystal structure of $Na_2[Cu(pn_2p)]_4Br_2(ClO_4)_4\cdot 3H_2O$ (**9**) is shown in Figure 8. Selected geometric parameters are given in the Supporting Information (Table S4).

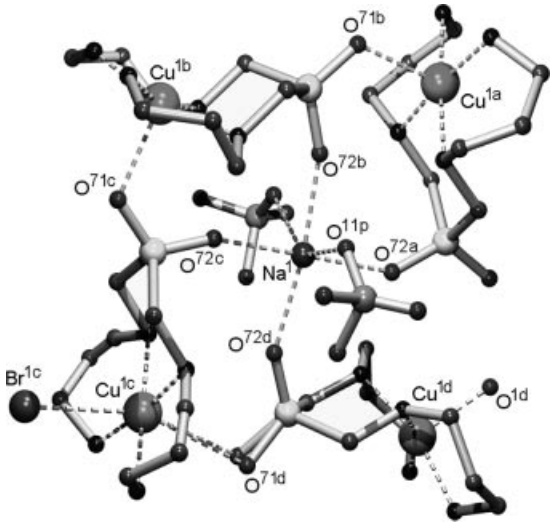

Figure 8. Complex framework found in the crystal structure of $Na_2[Cu(pn_2p)]_4Br_2(ClO_4)_4\cdot 3H_2O$ (**9**).

$[Ni_4(pn_2p)_4](ClO_4)_4\cdot 7H_2O$ (10)

In comparison with the previous complexes, the structure of this coplex is exceptional, as a structural unit is formed by an isolated $[Ni_4L_4]$ tetramer. The Ni^{2+} ions are connected by four ligand molecules to a supramolecular crown. Two nitrogen atoms of a propylenediamine fragment and one oxygen atom of a deprotonated phosphinate are coordinated to the metal ion in the meridional configuration. The second propylenediamine fragment and the second phosphinate oxygen atom are coordinated in the same way to the neighboring metal ion. The planes of those two groups of donor atoms are almost perpendicular. The remaining three positions around the metal ion are occupied by another ligand molecule. The Ni^{2+} ions can be viewed as the vertexes of an intermediate shape between a square and a tetrahedron, as their mutual position shows almost perfect D_{2v} symmetry with dihedral angles just between an ideal square and an ideal tetrahedron (Table 4; dihedral angles in the ideal tetrahedron are 70.5°, in square-planar geometry, the four angles are equal to 0°, and the remaining two are 180°). The positive charge is compensated for by four per-

Table 4. Dihedral angles [°] of the flattened tetrahedron formed by Ni^{2+} ions found in the structure of the $[Ni_4(pn_2p)_4]^{4+}$ cation.

Edge of the polyhedron	Angle /°	Square /°	Tetrahedron /°
Ni1···Ni2	51.9	0	70.5
Ni1···Ni3	103.4	180	70.5
Ni1···Ni4	52.0	0	70.5
Ni2···Ni3	52.3	0	70.5
Ni2···Ni4	103.4	180	70.5
Ni3···Ni4	51.7	0	70.5

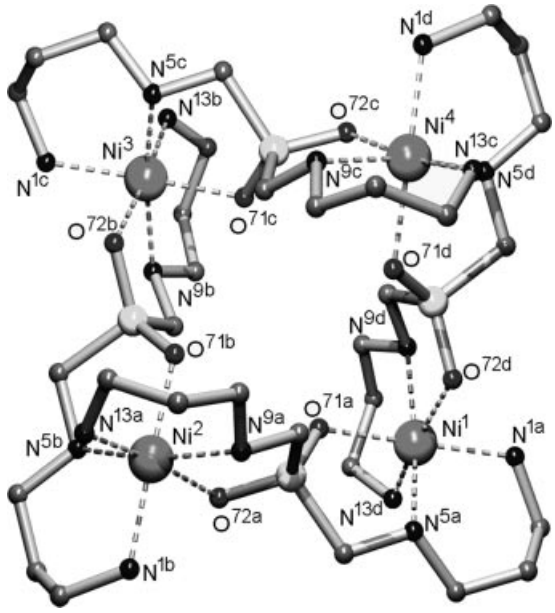

Figure 9. Structure of the $[Ni_4(pn_2p)_4]^{4+}$ complex cation.

chlorate anions, which are connected to water molecules by hydrogen bonds and ligand amino groups. The structure of the $[Ni_4(pn_2p)_4]^{4+}$ complex cation is presented in Figure 9, and selected geometric parameters are given in the Supporting Information (Table S5).

Conclusions

Two new symmetrical tetraazaphosphinic acids, bis[*N*-(2-aminoethyl)aminomethyl]phosphinic acid (Hen_2p) and bis[*N*-(3-aminopropyl)aminomethyl]phosphinic acid (Hpn_2p), were prepared by reaction of bis(chloromethyl)phosphinic acid with excess 1,2-diaminoethane or 1,3-diaminopropane. Their protonation constants and the stability constants of their complexes with Cu^{2+}, Ni^{2+}, and Zn^{2+} ions were determined by potentiometry. The presence of the electron-withdrawing phosphinic acid group decreases the basicity of the amino groups in the α-position in comparison with the linear tetraamines. The lower basicity results in the lower stability of the complexes with the divalent metal ions studied relative to that of the linear tetraamines containing the same number of bridging atoms between the amine groups. Chemical models for M^{2+}/Hen_2p systems are simpler than those of systems containing Hpn_2p, with a high preference for complexes with a M/L ratio of 1:1 as a result of the better stereochemical properties and the higher selectivity of Hen_2p. In single crystals of the complexes obtained from neutral and alkaline solutions, all nitrogen atoms show equatorial coordination, whereas the phosphinic acid group is coordinated to the neighboring metal center. A different motif was found in the structure of the $[Ni_4(pn_2p)_4](ClO_4)_4{\cdot}7H_2O$, where four Ni^{2+} ions and four ligand molecules form a cyclic supramolecular crown.

Experimental Section

Materials: Commercially available chemicals had synthetic purity and were used as received. Bis(chloromethyl)phosphinic acid (**1**) and isopropyl bis(chloromethyl)phosphinate (**2**) were prepared according to the reported procedures.[48,49] Elemental analyses were performed in the Institute of Macromolecular Chemistry (Academy of Sciences of the Czech Republic, Prague).

NMR Spectroscopy: ^1H (400.0 MHz), ^{13}C (100.6 MHz) and ^{31}P (161.9 MHz) NMR spectra were recorded with a Varian ^{UNITY}PLUS-400 spectrometer in 5 mm sample tubes. NMR experiments were performed at 298 K. For the measurements in D_2O, *tert*-butyl alcohol was used as an internal standard, the methyl signal being referenced to 1.2 ppm (^1H) and 31.2 ppm (^{13}C). For the measurements in $CDCl_3$, tetramethylsilane was used as an internal standard; the methyl signal was referenced to 0.0 ppm (^1H). The ^{31}P chemical shifts were measured with respect to 1% H_3PO_4 in D_2O as an external standard (substitution method).

Mass Spectrometry: Mass spectra were recorded by using a Bruker Esquire 3000 spectrometer equipped with an electrospray ion source and an ion trap. All measurements were carried out in the positive-ion mode.

General Procedure for Ligands Hen_2p and Hpn_2p: Bis(chloromethyl)phosphinic acid (**1**) (5.0 g, 30 mmol) was dissolved in diaminoalkane (3.0 mol). The solution was refluxed for 24 h. After removal of excess diaminoalkane in a rotary evaporator, the resulting oil was purified on a strong anion exchange resin (Dowex 1×8, 100–200 mesh, OH^--form, elution with H_2O followed with 20% aq. HCl) and a strong cation exchange resin (Dowex 50×4, 100–200 mesh, H^+-form, elution with H_2O followed with 5% aq. NH_3). After evaporation of the volatiles, the resulting oily products were dissolved in 30% HBr (20 mL) and treated with charcoal. After filtration, the volatiles were removed in a rotary evaporator, the residue was dissolved in water (5 mL), and the resulting solution was slowly dropped into anhydrous EtOH (800 mL) with vigorous stirring. After 3 h, the precipitate was filtered, washed with EtOH, and dried with P_2O_5 under reduced pressure.

Bis[*N*-(2-aminoethyl)aminomethyl]phosphinic Acid Trihydrobromide, $(H_4en_2p)Br_3$: Yield 9.8 g (72%). $C_6H_{22}Br_3N_4O_2P$ (452.95): calcd. C 15.91, H 4.90, Br 52.92, N 12.37; found C 16.02, H 4.86, Br 48.55, N 11.47. ^1H NMR (D_2O): δ = 3.34 (m, 8 H, NH_2–CH_2–CH_2–NH), 3.44 (m, 4 H, CH_2–P) ppm. ^{31}P NMR (D_2O): δ = 19.0 (p, $^2J_{PH}$ = 9.7 Hz) ppm. $^{13}C\{^1H\}$ NMR (D_2O): δ = 37.9 (s, NH_2–CH_2), 48.5 (d, $^3J_{CP}$ = 21.8 Hz, NH–CH_2–CH_2), 49.2 (d, $^1J_{CP}$ = 103.2 Hz, CH_2–P) ppm. MS: calculated for [M + Na^+] 233.2; found 233.6.

Bis[*N*-(3-aminopropyl)aminomethyl]phosphinic Acid Trihydrobromide, $(H_4pn_2p)Br_3$: Yield 10.0 g (69%). $C_8H_{26}Br_3N_4O_2P$ (481.00): calcd. C 19.98, H 5.45, N 11.65, Br 49.84; found C 20.35, H 5.44, N 11.11, Br 47.76. ^1H NMR (D_2O): δ = 2.03 (m, 4 H, CH_2–CH_2–CH_2), 3.02 (t, $^3J_{HH}$ = 8.0 Hz, 4 H, NH_2–CH_2–CH_2), 3.17 (t, $^3J_{HH}$ = 8.0 Hz, 4 H, NH–CH_2–CH_2), 3.26 (d, $^2J_{PH}$ = 10.0 Hz, 4 H, NH–CH_2–P) ppm. ^{31}P NMR (D_2O): δ = 19.7 (p, $^2J_{PH}$ = 9.9 Hz) ppm. $^{13}C\{^1H\}$ NMR (D_2O): δ = 25.2 (s, CH_2–CH_2–CH_2), 38.1 (s, NH_2–CH_2), 47.7 (d, $^1J_{CP}$ = 101.9 Hz, CH_2–P), 48.1 (s, NH–CH_2–CH_2) ppm. MS: calculated for [M + Na^+] 261.3; found 261.5.

Preparation of Single Crystals for X-ray Analysis

$(H_4en_2p)Cl_3$ (4): $(H_4en_2p)Br_3$ (0.10 g, 0.31 mmol) was evaporated with HCl (10 mL, 6 M). The resulting oil was dissolved in HCl (2 mL, 6 M). Colorless single crystals were prepared by slow vapor diffusion of EtOH into the solution.

$(H_4en_2p)[CuCl_4]Cl$ (5): $(H_4en_2p)Br_3$ (0.1 g, 0.31 mmol) and $CuCl_2{\cdot}2H_2O$ (0.053 g, 0.31 mmol) were dissolved in HCl (2 mL, 12 M). Volatiles were removed in a rotary evaporator, and the resulting oil was dissolved in H_2O (5 mL). Yellow single crystals of the product were obtained in 1 h.

$(H_4en_2p)[ZnCl_4]Cl$ (6): $(H_4en_2p)Br_3$ (0.10 g, 0.31 mmol) and $ZnCl_2$ (0.043 g, 0.31 mmol) were dissolved in HCl (2 mL, 12 M). Volatiles were removed in a rotary evaporator, and the resulting oil was dissolved in H_2O (5 mL). Colorless single crystals were obtained by slow evaporation over a week.

$Na_2(NH_4)_4[Cu(en_2p)]_4Br_4(PF_6)_6{\cdot}H_2O$ (7): $(H_4en_2p)Br_3$ (0.048 g, 0.11 mmol) and $CuCl_2{\cdot}2H_2O$ (0.018 g, 0.11 mmol) were dissolved in water (0.75 mL). The pH of the solution was increased to 8.5 by using NaOH (5% aq.), and a concentrated solution of NH_4PF_6 in EtOH (0.5 mL) was added. Blue single crystals were obtained by slow evaporation over two weeks.

$Na_{3/2}(NH_4)_2[Zn(en_2p)]_3Br_{5/2}(PF_6)_4{\cdot}3H_2O$ (8): $(H_4en_2p)Br_3$ (0.048 g, 0.11 mmol) and $ZnCl_2$ (0.015 g, 0.11 mmol) were dissolved in water (0.75 mL). The pH of the solution was increased to 8.0 by using NaOH (5% aq.), and a concentrated solution of NH_4PF_6 in EtOH (0.5 mL) was added. Colorless single crystals were obtained by slow evaporation over a week.

$Na_2[Cu(pn_2p)]_4Br_2(ClO_4)_4{\cdot}3H_2O$ (9): $(H_4pn_2p)Br_3$ (0.055 g, 0.11 mmol) and $CuCl_2{\cdot}2H_2O$ (0.019 g, 0.11 mmol) were dissolved

in water (0.75 mL). The pH of the solution was increased to 8.5 by using NaOH (5% aq.), and a concentrated solution of $NaClO_4$ in EtOH (0.5 mL) was added. Blue single crystals were obtained by slow evaporation over a week.

$[Ni_4(pn_2p)_4](ClO_4)_4·7H_2O$ (10): $(H_4pn_2p)Br_3$ (0.055 g, 0.11 mmol) and $NiCl_2·6H_2O$ (0.026 g, 0.11 mmol) were dissolved in water (0.75 mL). The pH of the solution was increased to 9.0 by using NaOH (5% aq.), and a concentrated solution of $NaClO_4$ in EtOH (0.5 mL) was added. Light blue single crystals were obtained from the mixture that was kept in a closed vial for a week.

Crystal Structure Determination: The selected crystals were mounted on glass fibers in random orientation by using silicone grease. Diffraction data were collected by using graphite-monochromated Mo-K_α radiation with an Enraf–Nonius KappaCCD diffractometer at 150(1) K [Cryostream Cooler (Oxford Cryosystems)] and analyzed with the HKL DENZO program package (ref.[50]). Cell parameters were determined from all data with the same program package.[50] The structure was solved by direct methods and refined by full-matrix least-squares techniques (SIR92,[51] SHELXL97[52]). The scattering factors used for neutral atoms were included in the SHELXL97 program. In the structures of $(H_4en_2p)Cl_3$ (**4**), $(H_4en_2p)[CuCl_4]Cl$ (**5**), and $(H_4en_2p)[ZnCl_4]Cl$ (**6**), all non-hydrogen atoms were refined anisotropically. The hydrogen atoms were localized in the difference map of electronic density and refined isotropically. In the structure of $Na_2(NH_4)_4[Cu(en_2p)]_4Br_4(PF_6)_6·H_2O$ (**7**), all non-hydrogen atoms of the complex units were refined anisotropically. The hydrogen atoms were placed in theoretical (C–H, N–H of amino groups) or original (O–H, N–H of ammonia cations) positions and treated by using a riding model with thermal parameters $U_{eq}(H) = 1.2U_{eq}(X)$. All copper(II) ions, phosphinate phosphorus and oxygen atoms, and bromide and sodium ions occupy the special positions (lying in the plane of symmetry). Two of the hexafluorophosphate anions were disordered. One was treated in two staggered positions (having axial fluorine atoms nondisordered, and equatorial ones with ca. 80:20 occupancies). All fluorine atoms of the second disordered hexafluorophosphate were refined in two positions in ca. 80:20 occupancies. More occupied fluorine atoms were refined anisotropically, less occupied atoms were refined isotropically. In the structure of $Na_{3/2}(NH_4)_2[Zn(en_2p)]_3Br_{5/2}(PF_6)_4·3H_2O$ (**8**), all non-hydrogen atoms were refined anisotropically. The hydrogen atoms were placed in theoretical (C–H, N–H of amino groups) or original (O–H, N–H of ammonia cations) positions and treated by using a riding model with thermal parameters $U_{eq}(H) = 1.2U_{eq}(X)$. All zinc(II) ions, phosphinate phosphorus and oxygen atoms, and bromide and sodium ions occupy special positions (lying in the plane of symmetry). Both hexafluorophosphate anions were disordered, and all their fluorine atoms were refined in two positions with occupancies of ca. 60:40 and ca. 50:50, respectively. To obtain reliable thermal parameters, one bromide and one sodium(I) ion were treated as half-occupied. In the structure of $Na_2[Cu(pn_2p)]_4Br_2(ClO_4)_4·3H_2O$ (**9**), all non-hydrogen atoms were refined anisotropically. The hydrogen atoms were placed in theoretical positions and treated by using a riding model with thermal parameters $U_{eq}(H) = 1.2U_{eq}(X)$. All copper(II) ions, phosphinate phosphorus and oxygen atoms, and bromide and sodium ions occupy special positions (lying in the plane of symmetry). Perchlorate oxygen atoms were disordered; the anion was found to be staggered in two positions with occupancies of ca. 70:30 (one oxygen atom was not disordered, the remaining three were disordered). The propylene backbone of one ligand molecule was refined in two positions with ca. 50:50 occupancies. Water oxygen atoms were treated as half-occupied to obtain reasonable thermal factors. In the structure of $[Ni_4(pn_2p)_4](ClO_4)_4·7H_2O$ (**10**), all non-hydrogen atoms were refined anisotropically. The hydrogen atoms belonging to the ligand molecules were localized in the difference map of electronic density and refined isotropically. Three perchlorate anions were disordered, and their oxygen atoms were refined with ca. 70:40–60:40 occupancies. Some water oxygen atoms were treated as half-occupied to obtain reliable thermal factors; hydrogen atoms belonging to cocrystallized water molecules were not found. Relatively high electronic maxima peaks

Table 5. Experimental data for the reported crystal structures (**4**, **5**, **6**, and **7**).

Parameter	**4**	**5**	**6**	**7**
Formula	$C_6H_{24}Cl_3N_4O_3P$	$C_6H_{22}Cl_5CuN_4O_2P$	$C_6H_{22}Cl_5N_4O_2PZn$	$C_{24}H_{90}Br_4Cu_4F_{36}N_{20}Na_2O_9P_{10}$
M	337.61	454.04	455.87	2416.64
Crystal system	monoclinic	monoclinic	monoclinic	monoclinic
Space group	Cc (No. 9)	Cc (No. 9)	Cc (No. 9)	$P2_1/m$ (No. 11)
a /Å	15.407(1)	8.3447(2)	8.1077(2)	12.9522(4)
b /Å	10.791(1)	19.7531(6)	19.6706(4)	17.6610(5)
c /Å	10.148(1)	10.4301(3)	10.6603(2)	16.9828(3)
β /°	116.151(4)	94.089(1)	94.2672(8)	91.5128(16)
V /Å^3	1514.48(16)	1714.86(8)	1695.43(6)	3883.44(18)
Z	4	4	4	2
D_c /g cm^{-3}	1.481	1.759	1.786	2.067
μ /mm^{-1}	0.714	2.147	2.332	3.498
$F(000)$	712	924	928	2396
θ range /°	2.80–27.48	3.40–27.50	2.82–27.51	1.20–27.49
Index ranges	$-19 < h < 19$; $-13 < k < 11$; $-13 < l < 13$	$-10 < h < 10$; $-21 < k < 25$; $-13 < l < 13$	$-10 < h < 10$; $-25 < k < 25$; $-13 < l < 13$	$-16 < h < 16$; $-22 < k < 22$; $-21 < l < 21$
Reflections total	2210	3321	3783	9041
Reflections observed [$I > 2\sigma(I)$]	2134	2975	3685	6268
Data; restraints; parameters	2210; 0; 249	3321; 2; 224	3783; 2; 225	9041; 0; 586
GOF	1.086	1.072	1.057	1.024
R_1, R_2 [$I \geq 2\sigma(I)$]	0.0258, 0.0238	0.0384, 0.0312	0.0346, 0.0336	0.0917, 0.0552
wR_1, wR_2 [$I \geq 2\sigma(I)$]	0.0612, 0.0593	0.0714, 0.0677	0.0857, 0.0846	0.1573, 0.1367
Max shift /e.s.d.	0.000	0.001	0.000	0.001
Highest diff. peaks/holes /e A^{-3}	0.198, –0.252	0.307, –0.441	2.418, –0.593	0.918, –2.217

Table 6. Experimental data of reported crystal structures (**8**, **9**, and **10**).

Parameter	**8**	**9**	**10**
Formula	$C_{18}H_{69}Br_{2.5}F_{24}N_{14}Na_{1.5}O_{9.5}P_7Zn_3$	$C_{16}H_{48}BrCl_2Cu_2N_8NaO_{14}P_2$	$C_{32}H_{102}Cl_4N_{16}Ni_4O_{31}P_4$
M	1737.07	939.44	1707.82
Crystal system	monoclinic	monoclinic	monoclinic
Space group	$C2/m$ (No. 12)	$P2_1/m$ (No. 11)	$P2_1/c$ (No. 14)
a /Å	24.3305(4)	13.2960(3)	19.7233(2)
b /Å	18.6827(2)	18.0898(5)	13.6071(2)
c /Å	14.0651(2)	15.3909(4)	25.5459(3)
β /°	110.9460(10)	110.4499(14)	92.1856(8)
V /Å^3	5970.93(14)	3468.55(15)	6850.94(15)
Z	4	4	4
D_c /g cm^{-3}	1.932	1.799	1.656
μ /mm^{-1}	3.195	2.708	1.424
F(000)	3463	1920	3576
θ-range /°	1.84–27.47	1.81–25.03	1.60–27.09
Index ranges	$-31 < h < 31$; $-24 < k < 24$; $-18 < l < 18$	$-15 < h < 15$; $-21 < k < 21$; $-18 < l < 18$	$-25 < h < 25$; $-17 < k < 17$; $-32 < l < 32$
Reflections total	7045	6334	15092
Reflections observed [$I > 2\sigma(I)$]	6142	4446	11683
Data; restraints; parameters	7045; 0; 474	6334; 0; 469	11683; 0; 1301
GOF	1.065	1.040	1.039
R_1, R_2 [$I \geq 2\sigma(I)$]	0.0848, 0.0771	0.1165, 0.0830	0.0655, 0.0455
wR_1, wR_2 [$I \geq 2\sigma(I)$]	0.2443, 0.2364	0.2529, 0.2288	0.1304, 0.1169
Max shift/e.s.d.	0.009	0.016	0.001
Highest diff. peaks/holes /e A^{-3}	1.859, –5.444	1.759, –2.462	1.251, –1.112

and holes in the structures of the compounds (**4**)–(**10**) are associated mainly with disordered hexafluorophosphate (or perchlorate) anions, as they are located in close proximity to phosphorus (or chlorine) atoms, respectively. Table 5 and Table 6 give the pertinent crystallographic data.

CCDC-627266 (**4**), -627267 (**5**), -627268 (**6**), -627269 (**7**), -627270 (**8**), -627271 (**9**), and -627272 (**10**) contain the supplementary crystallographic data for this paper. These data can be obtained free of charge from The Cambridge Crystallographic Data Centre via www.ccdc.cam.ac.uk/data_request/cif.

Potentiometric Titrations: The methodology of the potentiometric titrations and processing of the experimental data were similar to those previously reported.[9] Titrations were carried out in a vessel thermostatted at 25 ± 0.1 °C, at ionic strength I (KNO_3) = 0.1 mol dm^{-3}. Ligand-to-metal ratios were 1:1, 1:2, and 2:1. Titrations were carried out at least four times, each titration yielding about 40 data points. The water ion product, pK_w = 13.78, and stability constants of M^{2+}/OH^- systems were taken from ref.[53] The protonation constants β_n calculated are concentration constants and are defined by $\beta_n = [H_nL]/([H]^n \times [L])$ (pK_1 = logβ_1; pK_n = logβ_n – logβ_{n-1}); the stability constant are defined by $\beta_{pqr} = [M_pH_qL_r]/[M]^p \times [H]^q \times [L]^r$. The constants (with standard deviations) were calculated with the program OPIUM.[54] Throughout the paper, pH means –log[H^+]. As hydrobromides of the ligands slowly lose HBr upon standing, the stock solutions for potentiometry were prepared from freshly isolated materials. The ligand and the proton concentrations in the stock solution determined together with the calculation of the protonation constants, is in perfect agreement with a 1:3 ligand/HBr stoichiometry. In all systems, equilibrium was established quickly (< 20 s) at all data points.

UV/Vis Spectroscopy: Solution spectra were recorded with a Cary 1E (Varian) spectrometer in the 200–1100-nm range at room temperature. $NiCl_2 \cdot 6H_2O$ and ligand $(H_4pn_2p)Br_3$ (one equivalent) were dissolved in water, and the pH of the sample was adjusted with dilute KOH solution to a value of ca. 10, where the maximum abundance of the $[ML]^+$ species occurs according to the distribution diagram. Reflection spectra of the microcrystalline sample diluted with $BaSO_4$ were recorded with a Lambda 19 (Perkin–Elmer) spectrometer by using an integration sphere in the 200–1100-nm range at room temperature.

Supporting Information (see footnote on the first page of this article): Distribution diagrams of all studied systems are shown in Figures S1 and S2. Geometric parameters of coordination polyhedrons in the crystal structures are listed in Tables S1–S5. Colored structures and ORTEP representations of compounds **4**–**10** are shown in Figures S3 to S8.

Acknowledgments

Support from the Grant Agency of the Czech Republic (203/06/0467) and the Grant Agency of the Academy of Science of the Czech Republic (KAN201110651) is acknowledged. The work was carried out in the frame of COST D38 and the "Network of Excelence" projects EMIL (No. LSHC-2004–503569) and DiMI (No. LSHB-2005–512146).

[1] V. P. Kukhar, H. R. Hudson(Eds.), *Aminophosphonic and Aminophosphinic Acids. Chemistry and Biological Activity*, John Wiley and Sons, New York, **2000**.
[2] I. Lukeš, J. Kotek, P. Vojtíšek, P. Hermann, *Coord. Chem. Rev.* **2001**, *216–217*, 287–312.
[3] T. Kiss, I. Lázár. in *Aminophosphonic and Aminophosphinic Acids. Chemistry and Biological Activity* (Eds.: V. P. Kukhar, H. R. Hudson), John Wiley and Sons, New York, **2000**, ch. IX, pp. 285–326.
[4] J. E. Franz, M. K. Mao, J. A. Sikorski, *Glyphosate. A Unique Global Herbicide*, Oxford University Press, Oxford, **1997**.
[5] T. Kiss, E. Farkas, M. Jezowska-Bojczuk, H. Kozlowski, E. Kowalik, *J. Chem. Soc. Dalton Trans.* **1990**, 377–379.
[6] K. B. Yatsimirskii, L. B. Tsimbal, E. I. Sinyavskaya, *Zh. Neorg. Khim.* **1990**, *35*, 117–123.

[7] T. Kiss, M. Jezowska-Bojczuk, H. Kozlowski, P. Kafarski, K. Antczak, *J. Chem. Soc. Dalton Trans.* **1991**, 2275–2279.
[8] J. Rohovec, I. Lukeš, P. Vojtíšek, I. Císařová, P. Hermann, *J. Chem. Soc. Dalton Trans.* **1996**, 2685–2691.
[9] V. Kubíček, P. Vojtíšek, J. Rudovský, P. Hermann, I. Lukeš, *Dalton Trans.* **2003**, 3927–3938.
[10] M. Lukáš, M. Kývala, P. Hermann, I. Lukeš, D. Sanna, G. Micera, *J. Chem. Soc. Dalton Trans.* **2001**, 2850–2857.
[11] T. Glowiak, W. Sawka-Dobrowolska, *Acta Crystallogr., Sect. B* **1977**, *33*, 2648–2650.
[12] T. Glowiak, W. Sawka-Dobrowolska, *Acta Crystallogr., Sect. B* **1977**, *33*, 2763–2766.
[13] Z. Žák, J. Kožíšek, T. Z. Glowiak, *Z. Anorg. Allg. Chem.* **1981**, *477*, 221–224.
[14] W. Sawka-Dobrowolska, T. Glowiak, *Acta Crystallogr., Sect. C* **1983**, *39*, 345–347.
[15] T. Glowiak, *Acta Crystallogr., Sect. C* **1986**, *42*, 62–64.
[16] I. Lukeš, I. Císařová, P. Vojtíšek, K. Bazakas, *Polyhedron* **1995**, *14*, 3163–3166.
[17] J. F. Britten, C. J. L. Lock, Z. Y. Wang, *Acta Crystallogr., Sect. C* **1993**, *49*, 881–884.
[18] D. Parker, J. A. G. Williams, *J. Chem. Soc. Dalton Trans.* **1996**, 3613–3628.
[19] M. P. Lowe, S. J. Rettig, C. Orvig, *J. Am. Chem. Soc.* **1996**, *118*, 10446–10456.
[20] M. P. Lowe, P. Caravan, S. J. Rettig, C. Orvig, *Inorg. Chem.* **1998**, *37*, 1637–1647.
[21] M. S. Kovacs, V. Monga, B. O. Patrick, C. Orvig, *Dalton Trans.* **2006**, 31–38.
[22] J. Kotek, F. K. Kálmán, P. Hermann, E. Brücher, K. Binnemans, I. Lukeš, *Eur. J. Inorg. Chem.* **2006**, 1976–1986.
[23] K. Bazakas, I. Lukeš, *J. Chem. Soc. Dalton Trans.* **1995**, 1133–1137.
[24] J. Rohovec, M. Kývala, P. Vojtíšek, P. Hermann, I. Lukeš, *Eur. J. Inorg. Chem.* **2000**, 195–203.
[25] I. Lázár, A. D. Sherry, R. Ramasamy, E. Brücher, R. Király, *Inorg. Chem.* **1991**, *30*, 5016–5019.
[26] J. Huskens, A. D. Sherry, *Inorg. Chem.* **1996**, *35*, 5137–5143.
[27] J. Huskens, A. D. Sherry, *J. Am. Chem. Soc.* **1996**, *118*, 4396–4404.
[28] J. Huskens, A. D. Sherry, *J. Chem. Soc. Dalton Trans.* **1998**, 177–184.
[29] J. Huskens, D. A. Torres, Z. Kovacs, J. P. André, C. F. G. C. Geraldes, A. D. Sherry, *Inorg. Chem.* **1997**, *36*, 1495–1503.
[30] J. Kotek, P. Lebdušková, P. Hermann, L. Vander Elst, R. N. Muller, C. F. G. C. Geraldes, T. Maschmeyer, I. Lukeš, J. A. Peters, *Chem. Eur. J.* **2003**, *9*, 5899–5915.
[31] P. Lebdušková, J. Kotek, P. Hermann, L. Vander Elst, R. N. Muller, I. Lukeš, J. A. Peters, *Bioconjugate Chem.* **2004**, *15*, 881–889.
[32] J. Rudovský, J. Kotek, P. Hermann, I. Lukeš, V. Mainero, S. Aime, *Org. Biomol. Chem.* **2005**, *3*, 112–117.
[33] J. Rudovský, P. Hermann, M. Botta, S. Aime, I. Lukeš, *Chem. Commun.* **2005**, 2390–2392.
[34] J. Rudovský, M. Botta, P. Hermann, A. Koridze, S. Aime, *Dalton Trans.* **2006**, 2323–2333.
[35] J. Rudovský, M. Botta, P. Hermann, K. I. Hardcastle, I. Lukeš, S. Aime, *Bioconjugate Chem.* **2006**, *17*, 975–987.
[36] P. Lebdušková, A. Sour, L. Helm, E. Tóth, J. Kotek, I. Lukeš, A. E. Merbach, *Dalton Trans.* **2006**, 3399–3406.
[37] M. Försterová, I. Svobodová, P. Lubal, P. Táborský, J. Kotek, P. Hermann, I. Lukeš, *Dalton Trans.* **2007**, 535–549.
[38] K. P. Pullukkody, T. M. Norman, D. Parker, L. Royle, C. J. Broan, *J. Chem. Soc. Perkin Trans. 2* **1993**, 605–620.
[39] D. Parker, *Coord. Chem. Rev.* **2000**, *205*, 109–130.
[40] N. V. Nagy, T. Szabó-Plánka, G. Tircsó, R. Király, Z. Arkosi, A. Rockenbauer, E. Brücher, *J. Inorg. Biochem.* **2004**, *98*, 1655–1666.
[41] L. Xu, S. J. Rettig, C. Orvig, *Inorg. Chem.* **2001**, *40*, 3734–3738.
[42] G. Tircso, A. Benyei, R. Kiraly, I. Lazar, R. Pal, E. Brucher, *Eur. J. Inorg. Chem.* **2007**, 701–713.
[43] B. Song, T. Storr, S. Liu, C. Orvig, *Inorg. Chem.* **2002**, *41*, 685–692.
[44] A. E. Martell, R. M. Smith, *Critical Stability Constants*, Plenum Press, New York, **1974–1989**, vols. 1–6; NIST Standard Reference Database 46 (*Critically Selected Stability Constants of Metal Complexes*), Version 7.0, **2003**.
[45] W. N. Lipscomb, N. Sträter, *Chem. Rev.* **1996**, *96*, 2375–2433.
[46] N. V. Kaminskaia, Ch. He, S. J. Lippard, *Inorg. Chem.* **2000**, *39*, 3365–3373.
[47] R. D. Hanckock, *Acc. Chem. Res.* **1990**, *23*, 253–257.
[48] L. Maier, *Helv. Chim. Acta* **1969**, *52*, 827–845.
[49] L. Maier, *J. Organomet. Chem.* **1979**, *178*, 157–169.
[50] Z. Otwinowski, W. Minor, *HKL Denzo and Scalepack Program Package*, Nonius BV, Delft, **1997**. For a reference see: Z. Otwinowski, W. Minor, *Methods Enzymol.* **1997**, *276*, 307–326.
[51] A. Altomare, G. Cascarano, C. Giacovazzo, A. Guagliardi, M. C. Burla, G. Polidori, M. Camalli, *J. Appl. Crystallogr.* **1994**, *27*, 435.
[52] G. M. Sheldrick, *SHELXL97. Program for Crystal Structure Refinement from Diffraction Data*, University of Göttingen, Göttingen, **1997**.
[53] C. F. Baes Jr, R. E. Mesmer, *The Hydrolysis of Cations*, Wiley, New York, **1976**.
[54] M. Kývala, I. Lukeš, *International Conference, Chemometrics '95*, p. 63. Pardubice, Czech Republic, **1995**; the full version of *"OPIUM"* is available (free of charge) on http://www.natur.cuni.cz/~kyvala/opium.html.

Received: January 4, 2007
Published Online: June 27, 2007

